Sequence stratigraphy of the lower-middle Hueco transition interval (lower Permian, Wolfcampian), Robledo Mountains, New Mexico

G. H. Mack, K. A. Giles, and C. W. Durr

New Mexico Geology, v. 35, n. 2 pp. 27-37, Print ISSN: 0196-948X, Online ISSN: 2837-6420.
https://doi.org/10.58799/NMG-v35n2.27

This page is intentionally left blank to maintain order of facing pages.

Sequence stratigraphy of the lower-middle Hueco transition interval (lower Permian, Wolfcampian), Robledo Mountains, New Mexico

Greg H. Mack, Department of Geological Sciences, New Mexico State University, Las Cruces, New Mexico 88003;
Katherine A. Giles, Department of Geological Sciences, University of Texas at El Paso, El Paso, Texas 79968;
Corey W. Durr, Bureau of Land Management, 1800 Marquess Street, Las Cruces, New Mexico, 88005

Abstract

A 96-m-thick, mixed siliciclastic-carbonate interval spanning the boundary between the lower and middle members of the lower Permian (Wolfcampian) Hueco Formation in the southeastern Robledo Mountains, New Mexico, contains depth-sensitive lithofacies that allow delineation of sea-level cycles on the Robledo Shelf. Carbonate lithofacies include (1) fenestral dolomudstone (supratidal to high intertidal), (2) peloidal dolomudstone (low intertidal to lagoon), (3) foram packstone and grainstone (restricted marine), (4) intraclast, fossiliferous grainstone (tidal channel), and (5) fossiliferous packstone (open marine), whereas (6) shale (offshore marine) constitutes the only siliciclastic lithofacies. The presence of both siliciclastic and carbonate lithofacies may be related to sea-level change but may also have been influenced by paleoclimate, with carbonate sediment deposited during more arid periods and siliciclastic sediment deposited during more humid periods. Compared to the remainder of the Hueco Formation, the Robledo Shelf experienced more restricted marine conditions, was shallower, and was not traversed by rivers during deposition of the lower-middle Hueco transition.

Several scales of sea-level cyclicity are present within the lower-middle Hueco transition, including decimeter-to meter-scale upward-shallowing parasequences, decimeter- to meter-scale sequences primarily represented by interbeds of carbonate and shale, and meter- to dekameter-scale composite megasequences composed of deeper-water sets of sequences overlain by shallower-water sets of sequences. A rough estimate of the average duration of the sequences is about 87 k.y., which is consistent with a glacial-eustatic origin. The average duration of the composite megasequences (about 600 k.y.), however, is longer than the longest glacial-eustatic cycle (about 400 k.y.), suggesting the possible role of non glacial eustacy and/or tectonic subsidence as controlling factors.

Introduction

In March 2009 the Congress of the United States designated the southeastern part of the Robledo Mountains near Las Cruces as the Prehistoric Trackways National Monument to protect and enhance research on the remaining vertebrate tracks in the Permian Abo Tongue of the Hueco Formation (Figs. 1, 2, 3; Lucas and Heckert 1995). Exposed within and adjacent to the borders of the national monument are other geologically important features, including (1) three other members of the Permian Hueco Formation, (2) Laramide (latest Cretaceous–Eocene) faults, paleocanyons and their conglomeratic fill, and regionally extensive andesitic volcaniclastic rocks, (3) middle Cenozoic rhyolite sills, and (4) late Cenozoic faults, conglomerates, and basalts related to the Rio Grande rift (Seager et al. 2008; Fig. 4). These rocks and structures provide important insight into the geologic history of southern New Mexico and, like the Permian vertebrate trackways, are worthy of preservation and study.

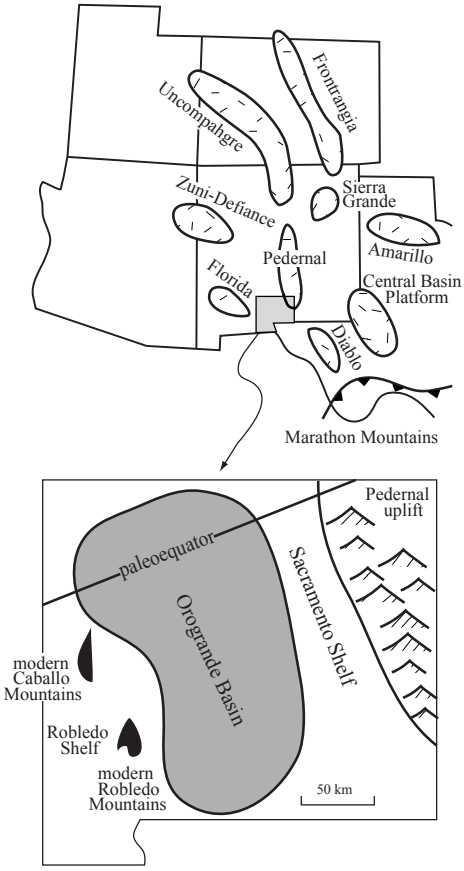

FIGURE 1—The Permian–Pennsylvanian Ancestral Rocky Mountains in the American Southwest. Inset shows the location of the modern Robledo and Caballo Mountains with respect to the Permian Robledo Shelf and Orogrande Basin, adapted from Kues and Giles (2004).

This study focuses on a unique 96-m-thick stratigraphic interval that straddles the contact between the lower and middle members of the Permian Hueco Formation. This interval, which is widely exposed within the national monument, consists of carbonate and siliciclastic strata that were deposited in environments ranging from offshore marine to supratidal. Decimeter- to dekameter-scale interbedding of these rocks provides a high-resolution record of Permian sea-level fluctuations at a variety of temporal scales. In addition, several of the facies display many of the features described on modern sabkhas of the Trucial Coast of the Persian Gulf, providing an excellent field laboratory for students. The goals of this study are (1) to interpret the depositional environments of the strata, (2) to use the stacking patterns and the nature of the contacts to interpret sea-level changes in the context of sequence stratigraphy, and (3) to consider the roles of paleoclimate and tectonics on sedimentary facies and stacking patterns.

Tectonic setting and stratigraphy

Pennsylvanian and lower Permian strata in New Mexico were deposited in intermontane basins that were complementary to uplifts of the Ancestral Rocky Mountains (Fig. 1). Located west of the Pedernal uplift was the Orogrande Basin, which contains approximately 1,600 m of Pennsylvanian and lower Permian sedimentary rocks (Kottlowski et al. 1956; Kottlowski 1963). The eastern margin of the Orogrande Basin (Sacramento Shelf) was tectonically active during Pennsylvanian and early Permian time (Pray 1961), and lower Permian conglomerates exposed in the Caballo Mountains suggest localized uplift along the western margin of the basin as well (Lawton et al. 2002; Seager and Mack 2003). The Orogrande Basin was bordered on the west by the Robledo Shelf, named for exposures in the Robledo Mountains (Kottlowski 1963). Lower Permian strata display an abrupt facies change from carbonate-rich sediment on the Robledo Shelf to more shale- and sandstone-rich sediment along the western margin of the Orogrande Basin (Seager et al. 1976). In addition to tectonism, sedimentation in the Orogrande Basin and on the Robledo Shelf was influenced by eustatic sea-level fluctuations (Stoklosa et al. 1998; Mack et al. 2003; Mack 2007) and changes in paleoclimate (Mack 2003, 2007).

Lower Permian stratigraphic terminology in this study conforms to the geologic map of the Robledo Mountains by Seager et al. (2008), who applied the terminology of Kottlowski (1963). This approach follows

precedence and allows future geologists to locate the members discussed here on the geologic map. In the Robledo Mountains, the Hueco Formation is divided into four mappable members, which in ascending order are the lower Hueco, middle Hueco, Abo Tongue, and upper Hueco (Fig. 2). Fusulinids in the lower part of the lower Hueco Member indicate an early Wolfcampian (Nealian) age (Wahlman and King 2002), but fusulinids are absent in the remainder of the formation in the Robledo Mountains. Conodonts and a marine invertebrate fauna from the Abo Tongue have been interpreted as late Wolfcampian (Lenoxian; Kues 1995; Kozur and LeMone 1995). Biostratigraphic data are currently insufficient to determine whether the Wolfcampian–Leonardian boundary exists within the upper Hueco member. The Hueco Formation in the Robledo Mountains contains three stratal packages deposited during relatively high sea level, separated by two intervals deposited during lower sea level (Fig. 2). Each of these large-scale intervals, which correspond to third-order cycles of Van Wagoner et al. (1990), is composed of smaller-scale sea-level cycles that are the focus of this study.

The lower and middle members of the Hueco Formation are separated by a 1.5-m-thick, ledge-forming marker bed composed of tan dolomudstone containing abundant dark-gray and brown chert nodules. However, the strata for 61 m below and 33.5 m above the marker bed, which are the subject of this study, are nearly identical, consisting of interbedded tan dolomudstones, gray limestones, and shales (Fig. 2). The base of the study interval is placed above a brown, pebbly sandstone in the lower interval of the lower Hueco member, whereas the upper contact is beneath thick-bedded, ledge- and cliff-forming, dark-gray limestones of the upper interval of the middle Hueco member (Fig. 2)

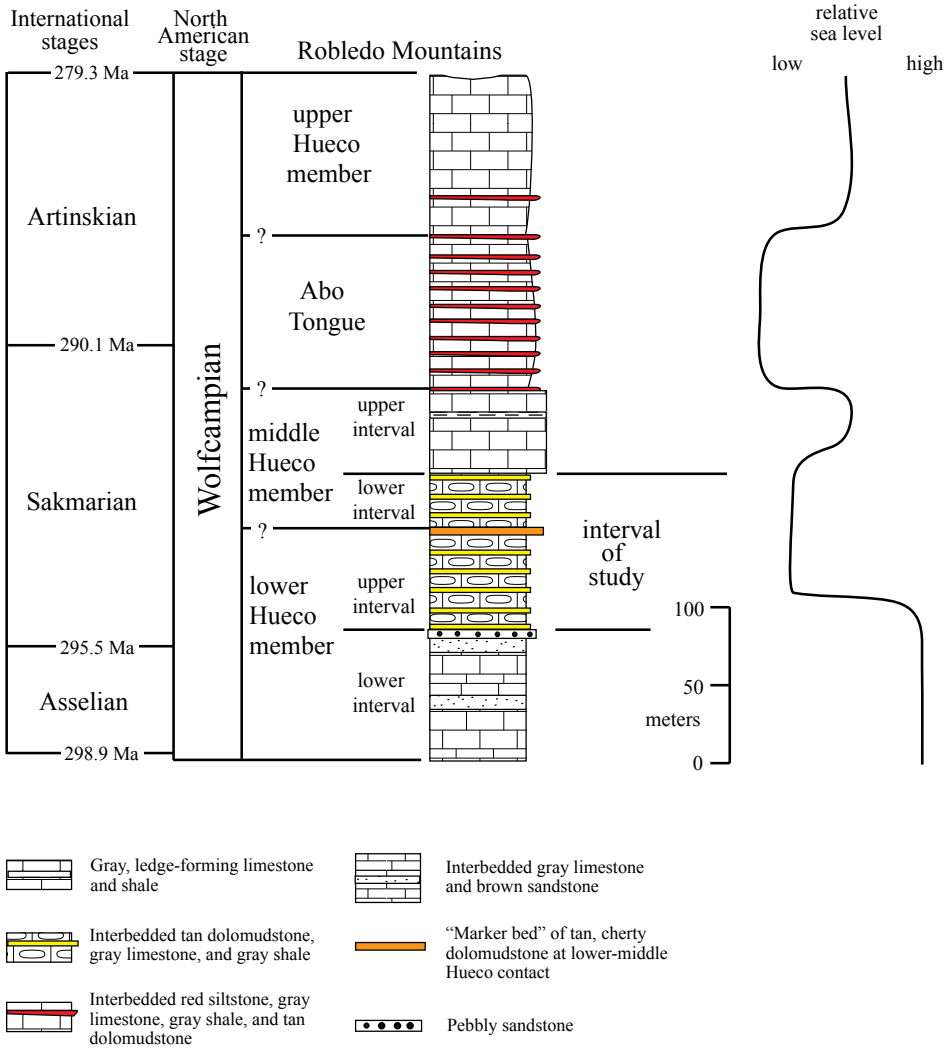

FIGURE 2—Generalized stratigraphy of the lower Permian Hueco Formation in the Robledo Mountains, adapted from Seager et al. (2008). International stages are from the International Chronostratigraphic Chart (2012). Currently, the exact correlation between the members of the Hueco Formation in the Robledo Mountains and the international stages is unknown.

Methods

Twelve partial stratigraphic sections were measured in the interval that straddles the lower and middle Hueco members in the Robledo Mountains (Durr 2010; Fig. 4). Where possible, key marker beds were traced on foot between the sections, which filled in covered intervals and established the lateral relationships of the facies. The 12 partial sections were ultimately combined into a single composite section (Fig. 5). In addition to standard field observations, 58 thin sections stained for calcite were examined with a polarizing microscope, and 64 crossbed paleocurrent measurements were collected from four stratigraphically different beds.

Lithofacies

The lower-middle Hueco transition in the study area is subdivided into six lithofacies. Carbonate lithofacies include (1) fenestral dolomudstone, (2) peloidal dolomudstone, (3) foram packstone and grainstone, (4) intraclast, fossiliferous grainstone, and (5) fossiliferous packstone. Shale (6) is the only siliciclastic lithofacies.

Fenestral dolomudstone lithofacies

The fenestral dolomudstone lithofacies consists of laterally continuous beds of tan to yellow dolomudstone. Bed thickness typically ranges from 10 and 50 cm, although a few beds are as much as 1.0 m thick. One of the thicker beds is very light tan to white, making it an excellent marker bed (Fig. 5, 3.2–4.2 m above base of section). Although generally unfossiliferous, some fenestral dolomudstones have scattered ostracodes, forams, sponge spicules, and calcispheres. One of the most common features in this lithofacies is fenestral fabric, which consists of millimeter- to centimeter-scale vugs, some of which are filled with sparry calcite or tan dolomudstone. Most of the fenestrae are elongate parallel to bedding (Fig. 6A), although a few bubble-shaped vugs are also present. Also common are millimeter-scale wavy laminae that may be disrupted laterally (Fig. 6B). In a few cases, the laminae are arranged into mounds a few centimeters high. Also in the fenestral dolomudstones are desiccation cracks (Fig. 6A), rounded intraclasts, flat-pebble intraclasts (Fig. 6C), spar-filled root traces (Fig. 6D), and millimeter- to centimeter-scale elongate voids with planar boundaries that may be spar filled (Fig. 6E). In addition, one bed has many nodules, averaging 2 cm in diameter, of white quartz containing inclusions of anhydrite (Fig. 5, 44.5 m above base of section). Petrographically, dolomite crystals are euhedral and less than 5 microns in diameter, and the rock has a locally distinctive clotted appearance (Fig. 6F).

The fenestral dolomudstone lithofacies displays most of the features that are diagnostic of the high intertidal to supratidal zones of modern carbonate tidal flats on the Trucial Coast of the Persian Gulf (Kinsman 1964; Evans 1966; Evans et al. 1969; Kendall and Skipwith 1969; Schneider

1975; Bathurst 1975; Shinn 1983). Wavy laminae are interpreted to be stromatolites produced by cyanobacterial mats, with most representing the flat-laminae type of Logan et al. (1964), although a few laterally linked hemispheroids are present as well. Evidence in fenestral dolomudstones for post-depositional subaerial exposure includes desiccation cracks, root traces, and fenestral fabric, the latter of which is interpreted to result from expansion and shrinkage of sediment, desiccation of cyanobacterial mats, and/or gas escape from decomposing cyanobacterial mats (Shinn 1968, 1983). Periodic storms and/or high tides probably deposited the intraclasts from both a seaward source and by ripping up sediment from within the high intertidal and supratidal environments, including flat-pebble intraclasts derived from desiccated cyanobacterial mats (Shinn 1983). Storms and high tides are probably also responsible for transporting the rare fossils into the high intertidal and supratidal environments, although ostracodes may have lived there.

Elongate voids with planar boundaries in the fenestral dolomudstones likely formed as displacive crystals of gypsum, which are common on sabkhas (supratidal flats) of the Trucial Coast (Kinsman 1964; Kendall and Skipwith 1969). Nodular anhydrite also was recognized on modern sabkhas of Abu Dhabi on the Trucial Coast (Curtis et al. 1963). The fact that dolomite in the study area is facies specific, being restricted to the fenestral and peloidal dolomudstone lithofacies, suggests that it may have formed shortly after deposition, as it does on the Trucial Coast and other modern carbonate shorelines. In these modern settings, dolomitization occurs at depths of a few meters or less from capillary draw or downward seepage of brines whose Mg/Ca ratios become elevated by precipitation of aragonite and gypsum/anhydrite (Adams and Rhodes 1960; Deffeyes et al. 1965; Illing et al. 1965; Shinn et al. 1965) and/or by the action of anaerobic, sulfate-reducing bacteria (Vasconcelos and McKenzie 1997).

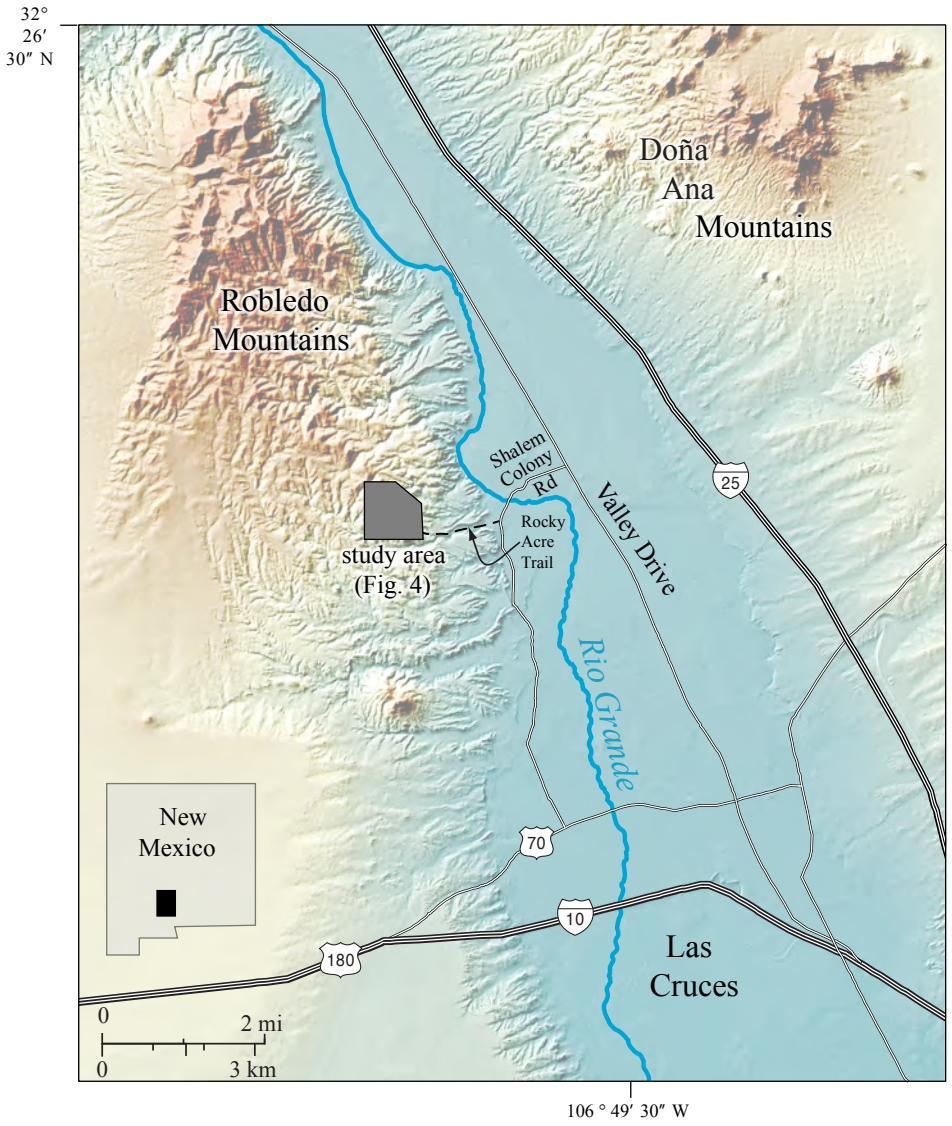

FIGURE 3—Location of the study area in the Robledo Mountains, northwest of Las Cruces, New Mexico.

Peloidal dolomudstone lithofacies

Laterally continuous beds of peloidal dolomudstone are light tan to light brown and range from 0.3 to 2.5 m thick (Fig. 7A). They consist primarily of peloids disseminated within a fine-grained dolomite matrix, whose crystals generally are less than 5 microns in diameter (Fig. 7B). Also present in many beds are variable numbers of ostracodes, sponge spicules, and well-rounded, detrital quartz silt and very fine quartz sand grains. White, siliceous sponge spicules are particularly common in a peloidal dolomudstone bed 66.3 m above the base of the section (Fig. 5). Rarely, the peloidal dolomudstones have fragmented echinoid spines, crinoid columnals, and bryozoans in thin (< 1 cm), discontinuous lenses or scattered throughout the bed. A few beds also display micro-scours (≤ 2 cm deep) and ripple cross-laminae (Fig. 7C). Simple, horizontal burrows are locally present on bedding planes, and several beds display light-tan and brown mottling that may have been produced by bioturbation. Pseudomorphs of calcite after swallowtail gypsum also are present in a few beds (Fig. 7D), as are dark-brown chert nodules. The peloidal dolomudstone that constitutes the marker bed at the contact between the lower and middle Hueco members is particularly chert rich (Fig. 5, 61.0–62.5 m above base of section).

Abundant microcrystalline matrix, peloids, and a sparse, low-diversity fauna indicate deposition of the peloidal dolomudstone lithofacies in a low-energy, highly restricted, shallow-marine environment (Enos 1983). Similar sediment is being deposited in modern lagoons and low intertidal flats along the Trucial Coast of the Persian Gulf (Kendall and Skipwith 1969), on the Bahama Bank (Newell et al. 1959; Purdy 1963), and in the Gulf of Batabano, Cuba (Bathurst 1975). The homogeneous nature of most of the beds of peloidal dolomudstone may be the result of extensive bioturbation, as is the case in the Trucial Coast (Shinn 1983; Enos 1983). Micro-scours, fossiliferous lenses, and ripple cross-laminae may have developed in the low intertidal flat (Shinn 1983) and/or on shallow banks like those in the lagoons of Abu Dhabi (Kendall and Skipwith 1969). Although current structures generally do not survive bioturbation in modern lagoons and low intertidal flats (Shinn 1983), burrowers may not have been as abundant in these environments during Permian time as they are today. Detrital silt and sand may have been supplied to the lagoon and low intertidal flats by streams, although excellent rounding of the sand grains suggests an eolian origin. The restrictive environment in which the peloidal dolomudstone was deposited was most likely due to periodic hypersalinity, based on calcite pseudomorphs after swallowtail

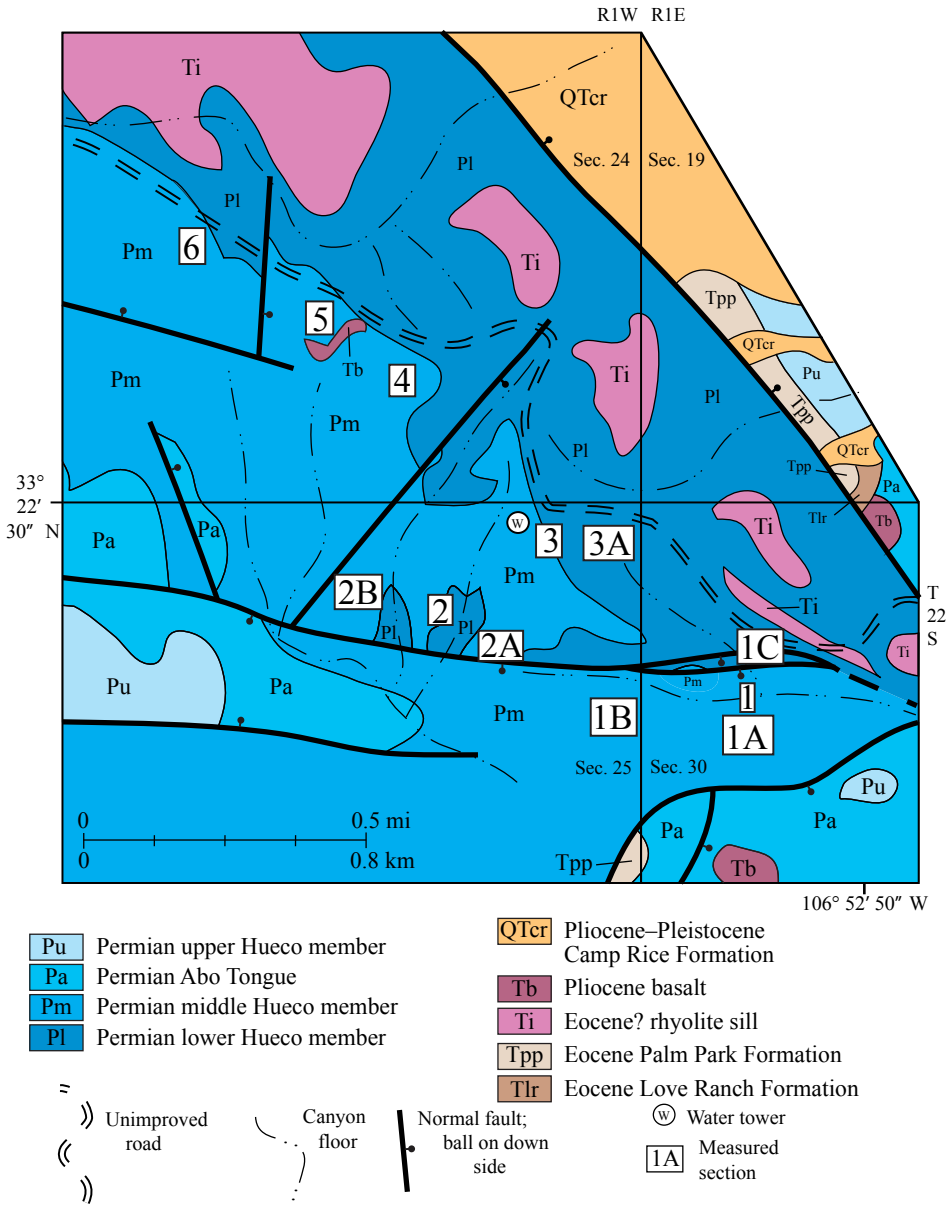

FIGURE 4—General geology and location of the partial measured sections used to construct the composite section of Figure 5. Geology is from Seager et al. (2008).

gypsum. Like the fenestral dolomudstone lithofacies, dolomitization of the peloidal dolomudstone facies also may have occurred shortly after burial (Enos 1983).

Most modern lagoons are protected from the open ocean by a barrier, such as reefs or ooid shoals (Bathurst 1975), or develop along shorelines with many small islands and/or highly irregular coastlines (Evans et al. 1969). However, highly restricted shallow-marine environments also may form on very broad, gentle ramps, as a result of damping of tidal and wave energy a long distance from open-ocean circulation (Shaw 1964; Irwin 1965; Ahr 1973). It is uncertain which of these applies to the study area, because it is not possible to reconstruct the shape of the ancient shoreline, nor identify the existence of small islands. Reefs and ooid shoals were not identified in rocks coeval to those of the study area in nearby mountain ranges, such as the Doña Ana and Organ Mountains (Seager et al. 1976; Seager 1981). However, the transition from the Robledo Shelf to the Orogrande Basin in early Wolfcampian time was interpreted as a ramp by Wilson and Jordan (1983), but it is not clear if their interpretation includes the stratigraphic interval of interest in this study.

Foram packstone and grainstone lithofacies

This lithofacies is composed of ledge- to cliff-forming beds of gray limestone from 0.3 to 2.5 m thick (Fig. 7E). The grain-supported limestone is dominated by forams, including uniserial, biserial, and milioline types, but no fusulinids are present (Fig. 7F). Also common are ostracodes, bivalves, echinoid spines and plates, small gastropods, and peloids. Rarely, a few intraclasts, ooids, and calcispheres are present as well. About half of the beds examined petrographically have micrite matrix, whereas the remainder have spar cement or local patches of both cement and matrix. Diffuse burrowing is evident within some beds; other beds display faint horizontal laminae. Many of the beds, particularly those in the upper part of the stratigraphic section, have numerous dark-brown to black chert nodules that are elongate parallel to bedding.

The abundance of fossils but the paucity of invertebrate filter feeders suggest that the foram packstone and grainstone lithofacies was deposited in a moderately restricted marine environment (Enos 1983; Wilson and Jordan 1983). Micrite matrix implies little or no current activity, whereas those beds with spar cement were probably winnowed by currents. The foram packstone and grainstone lithofacies may have been deposited seaward of the peloidal dolomudstone lithofacies in an environment more hospitable to benthic life. For example, on the shallow-marine ramp of the southern Persian Gulf, seaward of the coast of Abu Dhabi (Evans and Bush 1969), there is fine-grained, fossiliferous sediment with a fauna similar to that of the foram packstone and grainstone lithofacies.

In some other modern carbonate environments, however, foram-rich sediment is deposited in lagoons and is laterally equivalent to poorly fossiliferous, peloid- and micrite-rich sediment. In the Gulf of Batabano, Cuba, a peloid-foram-molluscan assemblage is being deposited in turbulent water, seaward of a micrite- and peloid-rich facies (Bathurst 1975). In the lagoon off the coast of Belize, foram-rich sediment grades into a micrite-peloid facies in a direction parallel to the shoreline (Purdy 1974). These latter two examples raise the possibility that the foram packstone and grainstone lithofacies and the peloidal dolomudstone lithofacies were deposited in different parts of the same lagoon or ramp. The interpretation that the foram packstone and grainstone lithofacies was deposited in deeper water than the peloidal dolomudstone lithofacies is preferred in this study, because there is no field evidence that the two lithofacies were laterally equivalent, the foram packstone and grainstone beds are not dolomitized, and beds of foram packstone and grainstone are not gradationally overlain by high intertidal to supratidal fenestral dolomudstones, as is commonly the case for beds of peloidal dolomudstone. However, the possibility that peloidal dolomudstone and foram packstone and grainstone were deposited at a similar depth in the same lagoon or shallow ramp cannot be precluded

Intraclast, fossiliferous grainstone lithofacies

Thirteen beds of intraclast, fossiliferous grainstone ranging from 0.3 to 3.0 m thick are recognized in the study area (Fig. 5). The laterally discontinuous beds have horizontal tops and erosive, convex-downward bases. The intraclast, fossiliferous grainstones

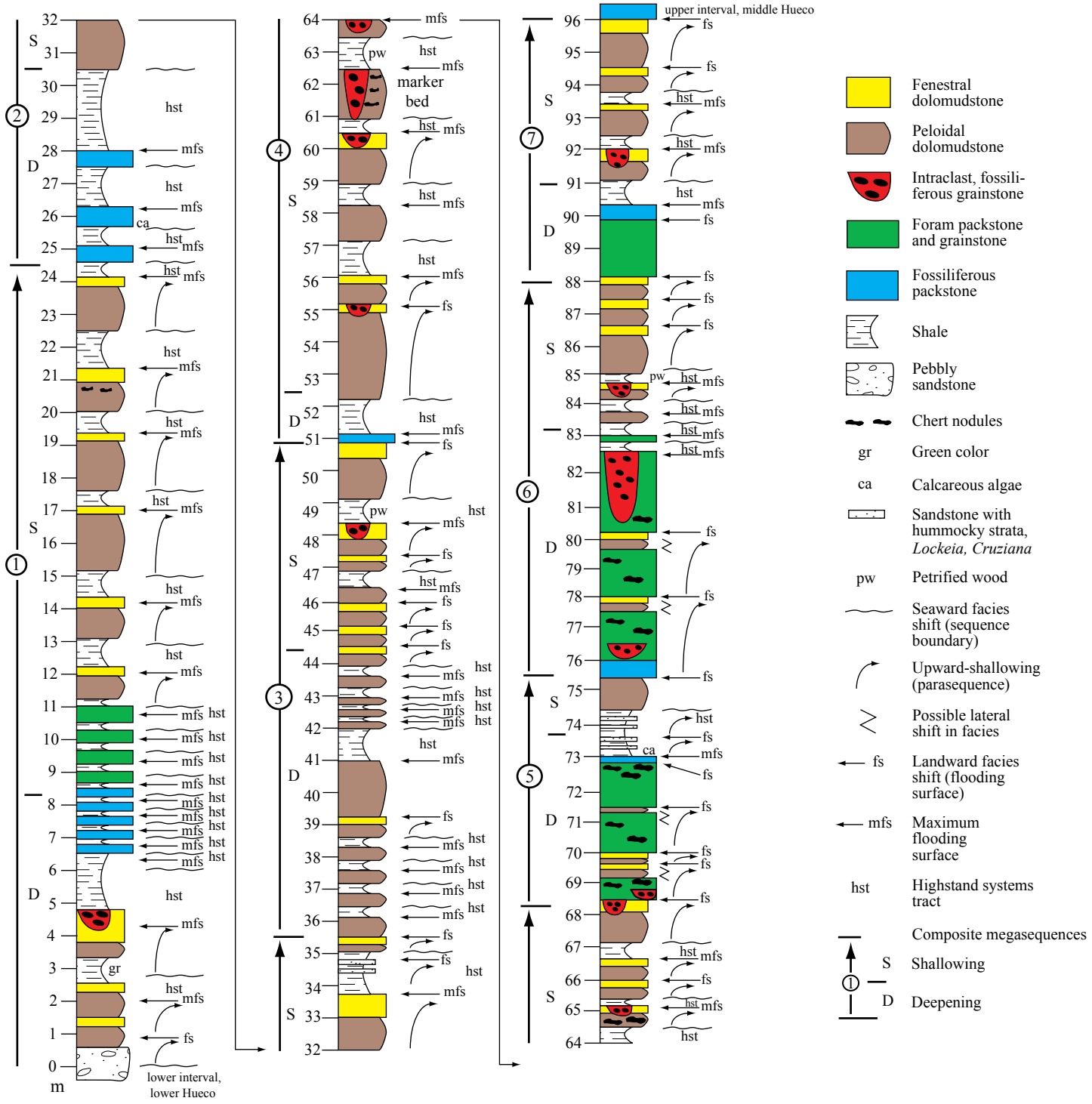

FIGURE 5—Composite stratigraphic section of the lower-middle Hueco transition in the Robledo Mountains.

truncate fenestral dolomudstone, peloidal dolomudstone, and foram packstone and grainstone lithofacies (Fig. 8A). The most common allochems are intraclasts, which are composed of limestone and dolomudstone, the latter displaying textures similar to those of the fenestral dolomudstone and peloidal dolomudstone lithofacies. Fossil fragments are also common and include ostracodes, bivalves, gastropods, brachiopods, forams, echinoid spines and plates, echinoderm columnals, and bryozoans. Many of the more complete shells are filled with micrite, whereas three beds contain abundant articulated spiriferid brachiopods (Fig. 5, 55.0, 62.0, and 81.5 m above base of section). Less common are ooids and detrital quartz sand, although one bed at 60.5 m above the base of the section shows a southward increase in ooids between measured sections 5 and 1 (Figs. 4 and 5). Most of the beds lack internal layering or are weakly horizontally laminated, but four beds have meter-scale planar crossbeds (Fig. 5, 55.0, 62.0, 81.5, and 92.0 m above the base of the section; Fig. 8B). Crossbed paleocurrent measurements from these beds show strong bipolarity to the northwest and southeast (Fig. 9). All of the beds examined petrographically have spar cement and a few silicified fossils.

The intraclast, fossiliferous grainstones were deposited in tidal channels, based on basal erosional truncation, channel morphology, abundant intraclasts, and bipolar crossbeds. Because the channels truncate fenestral dolomudstones, peloidal dolomudstones, and foram packstones and grainstones, they probably traversed the supratidal, intertidal,

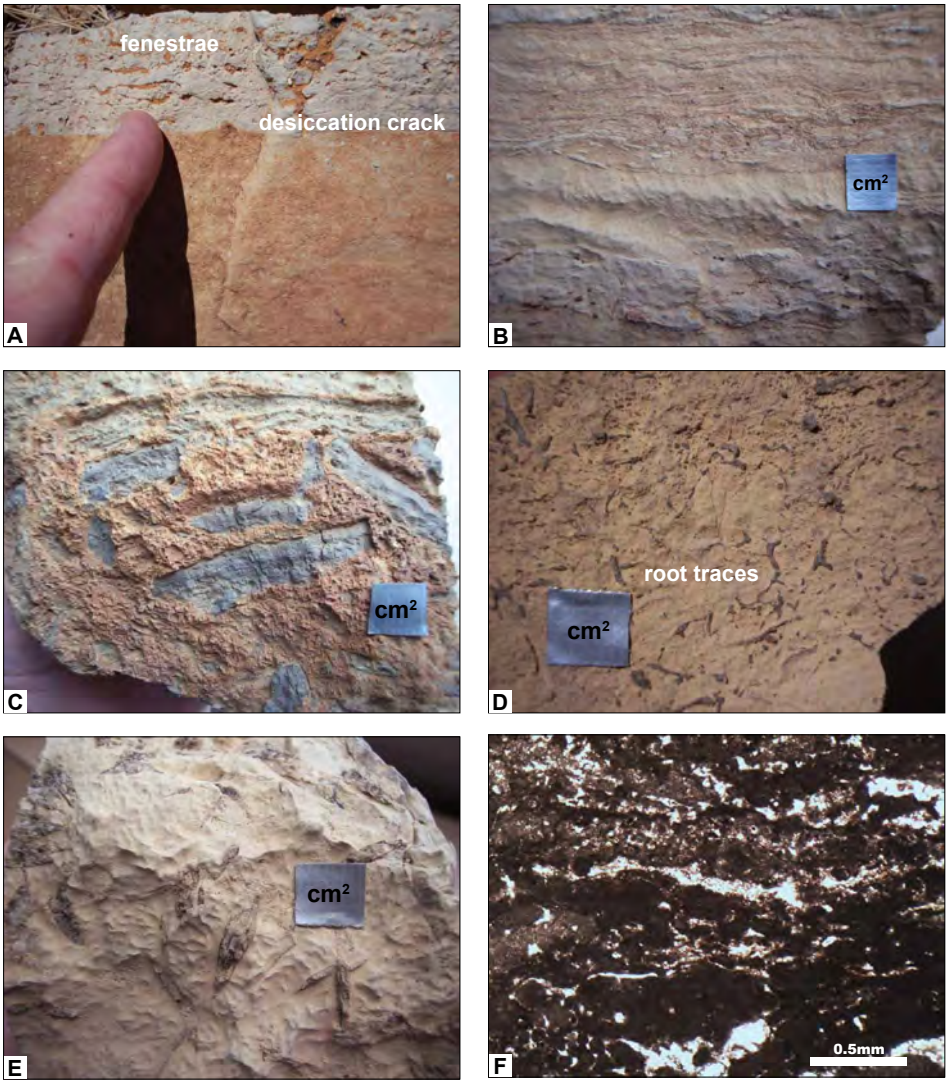

FIGURE 6—Photographs of fenestral dolomudstone lithofacies. **A**—Fenestrae and a desiccation crack overlying peloidal dolomudstone. Finger is 2 cm wide at tip. **B**—Wavy laminar stromatolite, which is locally brecciated. Scale is 1 cm^2. **C**—Gray flat-pebble intraclasts. Scale is 1 cm^2. **D**—Spar-filled root traces. Scale is 1 cm^2. **E**—Elongate, spar-filled vugs with planar boundaries, which are interpreted to have originally been displacive crystals of gypsum. Scale is 1 cm^2. **F**—Photomicrograph under uncrossed nicols showing fenestral fabric and clotted texture.

and shallow subtidal zones, similar to those along the Abu Dhabi coast (Kendall and Skipwith 1969; Evans et al. 1969; Bathurst 1975) and in the Bahamas (Bathurst 1975). The ooid-rich bed may have formed at the mouth of a tidal channel as a tidal ooid delta, such as those in Abu Dhabi (Evans and Bush 1969). Most of the fossils were disarticulated and broken during transport, but the articulated spiriferid brachiopods may have lived in the channel. The bipolar character of the cross-beds suggests that ebb and flood tides were of subequal velocities, which is consistent with the combination of limestone intraclasts that probably were derived from a seaward direction and dolomudstone intraclasts derived from the lagoon and intertidal-supratidal flat. The presence of dolomudstone intraclasts in the tidal channels also supports the idea of early dolomitization of supratidal, intertidal, and lagoonal dolomudstone.

Fossiliferous packstone lithofacies

The least common of the carbonate lithofacies is fossiliferous packstone, which consist of beds of gray limestone from 0.2 to 0.5 m thick (Fig. 5). This lithofacies has, in addition to those fossils present in the foram packstone and grainstone lithofacies, many brachiopods, bryozoans, echinoderm columnals, and calcareous algae (Fig. 8C). Although most of the calcareous algae exist as single, isolated fragments of phylloid algae, two of the beds have small (<30 cm diameter, <10 cm high) mounds of calcareous red algae (Fig. 5, 25.7 m, 73.1 m; Scholle and Ulmer-Scholle 2003). Many of the fossils have micritized rims or are encrusted with forams. All of the beds examined petrographically have micrite matrix, locally neomorphosed to microspar. Dark-gray chert nodules are locally present but are not abundant. In addition, a few beds exhibit normal grading of fossils and indistinct hummocky stratification.

Micrite matrix and a highly diverse fauna dominated by invertebrate filter feeders are indicative of a low-energy, normal-marine environment (Wilson and Jordan 1983). The presence of red algae, although not ubiquitous, suggests periods of cooler than normal water and/or unusually high nutrient content (Mutti and Hallock 2003). Graded beds and hummocky stratification indicate that the sediment was periodically reworked by storms. The open-marine character of the fossiliferous packstone lithofacies suggests deposition seaward of the foram packstone and grainstone lithofacies and the peloidal dolomudstone lithofacies.

Shale lithofacies

Shale commonly exists as covered slopes within the study area, although lateral tracing of these intervals verified the correct lithology. The shale is fissile or platy in fabric and dark gray or olive gray, although a green shale is present in the lower part of the section (Fig. 5, 2.0 m). The shale intervals range in thickness from a few centimeters to 2.5 m. Invertebrate fossils are very rare and restricted to ostracodes and bivalves, although finely macerated plant debris is common in the darker beds. In addition, dark-brown to black pieces of petrified wood 5–15 cm in diameter are present in three of the shale beds (Fig. 5, 48.5 m, 63.0 m, 84.8 m). Two other shale beds have thin (5–20 cm), tan to brown, very fine grained sandstones or siltstones that display hummocky stratification overlain by symmetrical ripple marks (Fig. 5, 34.8 m, 73.8 m). Many of the sandstones and siltstones also have trace fossils of *Cruziana*, *Rusophycus*, and *Planolites striatus* on the undersides of the beds (convex hyporelief; Fig. 8D) and molds of bivalves (*Lockeia*) in concave hyporelief.

Most of the shale beds were deposited in an offshore marine environment below storm wave base (Howard and Reineck 1981). The organic matter in the darker shales suggests the sea floor was periodically poorly oxygenated. Those two shale intervals with thin interbeds of sandstone and siltstone were deposited between normal wave base and storm wave base, based on the presence of hummocky stratification. Trace fossils in convex hyporelief in the sandstones and siltstones formed by organisms burrowing into or walking on a muddy surface, followed by infilling of the depressions with storm sands or silts. Trace fossils of this type require a firm mud substrate, which may have resulted from dewatering during compaction or incipient cementation due to slow sedimentation rates (Wetzel and Aigner 1986).

Sequence stratigraphy and paleoclimate

The fundamental concepts of sequence stratigraphy were developed using seismic reflection profiles on continental margins, where it is possible to trace unconformities and stratal onlap, offlap, and downlap on a basin-wide scale (Vail et al. 1977; Van Wagoner et al. 1988). Rarely is it possible in outcrop to confidently correlate erosional surfaces and stratal relationships over distances comparable to those of seismic lines. Consequently, sequence stratigraphy in outcrop relies upon facies stacking patterns and their Waltherian characteristics to interpret sequence boundaries and systems tracts (Van Wagoner et al. 1990). Implicit in this approach is establishing the relative depth of marine facies that existed within a basin. This can be problematic in Pennsylvanian and Permian rocks of the midcontinent and American Southwest, because of interbedding of carbonate and siliciclastic facies, types of sediment that are not commonly deposited together in modern environments.

The traditional idea is that clay and silt are transported seaward as buoyant plumes, bypassing nearshore carbonate environments and ultimately being deposited in deep water. In this model, the marine shale was deposited during maximum transgression, and eustatic sea-level change is responsible for the interbedding of siliciclastic and carbonate beds (Heckel 1977, 1980). In contrast, changes in paleoclimate could have resulted in alternating carbonate and siliciclastic sedimentation through time (Tandon and Gibling 1994; Miller et al. 1996; Rankey 1997). In the context of their studies of Permian–Pennsylvanian cycles, Cecil (1990), Soreghan (1997), and Olszewski and Patzkowsky (2003) suggested that the carbonate parts of cycles were deposited during relatively drier periods, whereas siliciclastic parts of cycles were due to wetter conditions.

The role of paleoclimate in lower-middle Hueco deposition

Although paleoclimatic indicators in the lower-middle Hueco transition in the Robledo Mountains are sparse, they generally conform to the paleoclimatic model cited above. Indicative of arid climate within the carbonate facies are calcite pseudomorphs after gypsum and nodular anhydrite. In contrast, the influx of clay, silt, and sand into the sea during deposition of the shale lithofacies argues for higher detrital sediment yields, requiring greater amounts of precipitation and runoff than during carbonate deposition. Moreover, fine plant debris and petrified wood in the shale lithofacies imply significant vegetation, including trees, in the catchment areas.

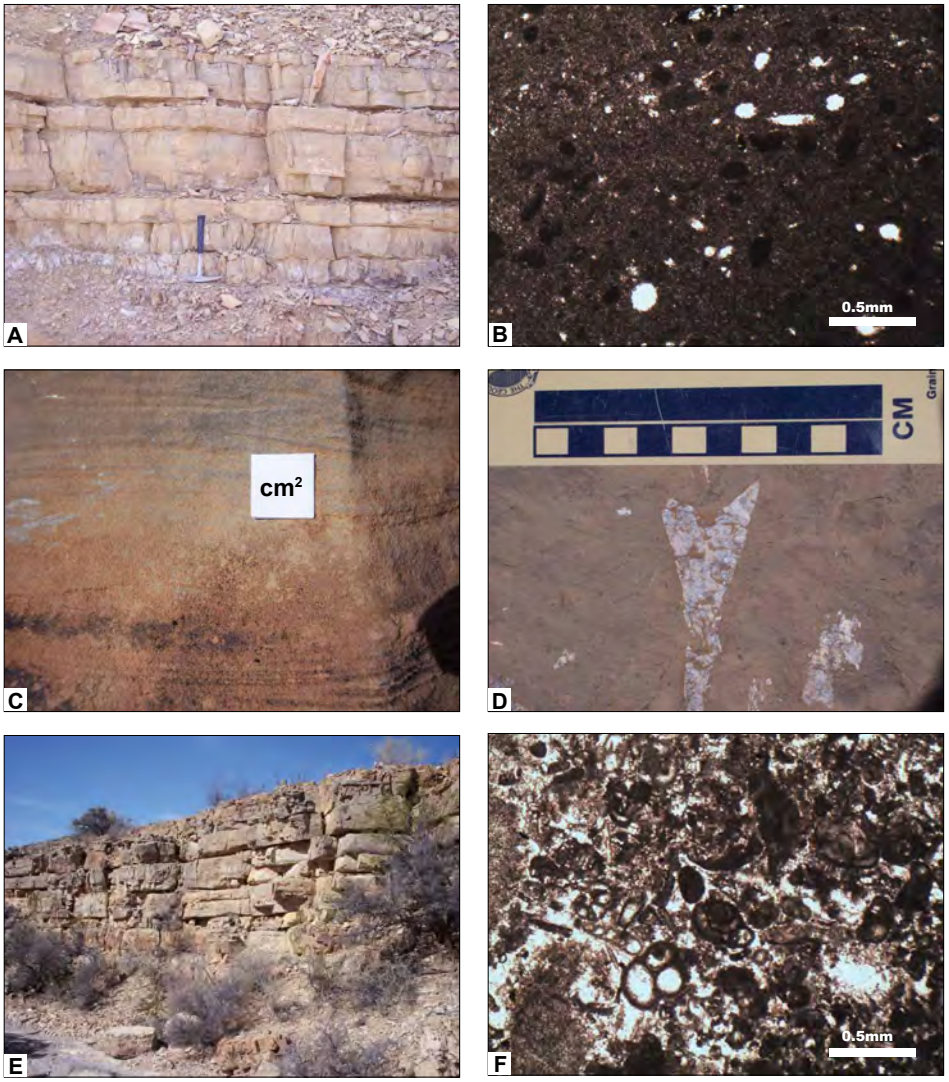

FIGURE 7—Photographs of peloidal dolomudstone and foram packstone and grainstone lithofacies. **A**—Interbedded peloidal dolomudstone and shale. Hammer is 32 cm long. **B**—Photomicrograph under uncrossed nicols showing peloids and white sponge spicules in peloidal dolomudstone lithofacies. **C**—Small-scale ripple cross-laminae in peloidal dolomudstone lithofacies. Scale is 1 cm^2. **D**—Calcite pseudomorph after displacive crystal of swallowtail gypsum in peloidal dolomudstone lithofacies. Scale is divided into centimeters. **E**—Upper half of outcrop, which is 4.5 m thick, is composed of gray beds of foram packstone and grainstone, whereas the lower part of the outcrop consists of tan peloidal dolomudstone beds. **F**—Photomicrograph under uncrossed nicols of foram packstone and grainstone lithofacies.

Waltherian relationships

Despite the fact that the shale and carbonate lithofacies may not have been deposited at the same time on the Robledo Shelf, it is still possible to place them in a Waltherian context. Among the carbonate lithofacies, the fenestral dolomudstone was the shallowest and the fossiliferous packstone the deepest (Fig. 10). Peloidal dolomudstone was probably shallower than foram packstone and grainstone, although they may have been lateral equivalents of one another in the same shallow lagoon or ramp. Intraclast, fossiliferous grainstones truncate fenestral dolomudstones, peloidal dolomudstones, and foram packstones and grainstones, indicating that tidal channels spanned the depth from supratidal to shallow, restricted marine.

The shale lithofacies was deposited below storm wave base or, in two cases, between normal and storm wave base on a poorly oxygenated sea floor and represents deeper water than the fenestral dolomudstone, peloidal dolomudstone, foram packstone and grainstone, and intraclast, fossiliferous grainstone lithofacies. Less certain is the depth of the shale lithofacies compared to the fossiliferous packstone lithofacies, although the presence of storm deposits and calcareous algae in many beds of fossiliferous packstone suggests that they were deposited in shallower water than most of the shales.

Parasequences and flooding surfaces

Carbonate lithofacies in the study area commonly display decimeter- to meter-scale, upward-shallowing parasequences (Fig. 11A)

that were created by seaward progradation of lithofacies that were originally adjacent to each other (Waltherian shift). The most common carbonate parasequence involves vertical stacking of fenestral dolomudstone above peloidal dolomudstone, which represents seaward progradation of supratidal to high intertidal sediment over lagoonal to low intertidal sediment (Figs. 5, 10, and 11A1). Vertical stacking of peloidal dolomudstone above foram packstone and grainstone (Fig. 11A2) may also be a parasequence if the two lithofacies were deposited at different depths. It is also possible, as discussed above, that these two lithofacies were deposited at nearly the same water depth, such that their juxtaposition is the result of lateral shifting of lithofacies and not a relative sea-level change. The third and fourth types of carbonate parasequences record upward shallowing, even if the juxtaposition of peloidal dolomudstone above foram grainstone and packstone represents a lateral lithofacies shift, because of the presence of fenestral dolomudstone capping each parasequence (Fig. 11A3, 4).

Each carbonate parasequence is sharply overlain by a flooding surface that indicates a relative rise in sea level. In many cases, the deeper-water lithofacies above the flooding surface has at its base a thin (<10 cm) interval of rip-up clasts derived from the underlying lithofacies, which is interpreted as a transgressive lag created by erosion during sea-level rise (Fig. 8E). However, in those cases where peloidal dolomudstone is present above the flooding surface, there is little evidence for erosion, probably because of the absence of strong current and wave activity in the lagoon.

Two intervals of shale (Fig. 5, approximately 34.5 and 73.5 m above base of composite section) contain upward-thickening beds of very fine sandstone deposited by storms. The storm beds are separated by thin (< 20 cm) shales, but each package of upward-thickening storm sands is sharply overlain by shale lacking interbedded sandstone. The storm-bed-bearing intervals are interpreted as upward-shallowing parasequences, overlain by a flooding surface (Van Wagoner et al. 1990; Fig. 11).

FIGURE 8—Photographs of intraclast, fossiliferous grainstone, fossiliferous packstone, and shale lithofacies, as well as transgressive lag and firmground. **A**—Upper gray bed of intraclast, fossiliferous grainstone truncates a bed of peloidal dolomudstone. Hammer is 32 cm long. **B**—Crossbeds and light-colored intraclasts in intraclast, fossiliferous grainstone lithofacies. Hammer is 32 cm long. **C**—Photomicrograph under uncrossed nicols of fossiliferous packstone, showing bryozoans and peloids in a partially recrystallized micrite matrix. **D**—Underside of bed of hummocky-stratified, fine-grained sandstone with *Cruziana* burrows in the shale lithofacies. Scale is 1 cm^2. **E**—Bedding plane view of a transgressive lag of intraclasts at the base of a bed of foram packstone and grainstone that overlies a bed of fenestral dolomudstone. Hammer head is 17 cm long. **F**—Bedding plane view of the heavily bioturbated top of a bed of fossiliferous packstone, defining a firmground and maximum flooding surface. Hammer is 32 cm long.

Carbonate-shale sequences

The most common stacking pattern in the lower-middle Hueco transition consists of interbedded carbonate and shale (Fig. 11B). Similar interbeds in lower Permian strata of Nebraska were interpreted by Olszewski and Patzkowsky (2003) as high-order sequences, based on many features that are also present in the lower-middle Hueco transition. Olszewski and Patzkowsky (2003) defined "nearshore" and "offshore" carbonate-shale cycles, with only the latter present in the lower-middle Hueco transition. In their "nearshore cycles," paleosols are present in marine shales directly beneath carbonate beds. The paleosols indicate exposure of the shales during sea-level fall and define a sequence boundary. Marine shales in the "offshore cycles" lack paleosols, but the sharp contact between the shale and overlying carbonate still constitutes a sequence boundary that involved a sea-level fall that did not expose the marine shale (Olszewski and Patzkowsky 2003). This interpretation is supported in the lower-middle Hueco transition not only by the sharp contact between offshore marine shale and overlying peloidal dolomudstone (lagoon, low intertidal) or foram packstone and grainstone (restricted marine), but by the fact that these carbonate lithofacies were deposited in much shallower water than the offshore marine shale, such that their vertical juxtaposition represents a non-Waltherian, seaward shift in lithofacies and, consequently, a sequence boundary. The sharp contact between fossiliferous packstone (normal marine) and underlying offshore marine shale is also considered to be a sequence boundary, although a difference in water depth between the two facies is not as well established.

In the model of Olszewski and Patzkowsky (2003), the marine carbonate interval directly overlying the sequence boundary represents the transgressive systems tract, whereas the bioturbated top of the carbonate interval constitutes the maximum flooding surface (Fig. 11B). In the lower-middle Hueco transition the transgressive systems tract is commonly represented by a single bed of carbonate, although there are cases in which several stacked parasequences constitute the transgressive systems tract. In most cases, the

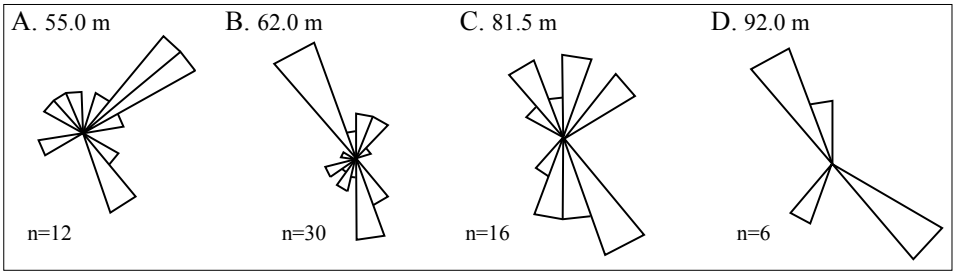

FIGURE 9—Planar-crossbed paleocurrent measurements from four beds of the intraclast, fossiliferous grainstone lithofacies. The rose diagram is in 15° intervals beginning at due north; "n" refers to the number of measurements per bed. The stratigraphic position of the beds in meters above the base of the composite section of Figure 5 is shown for each rose diagram.

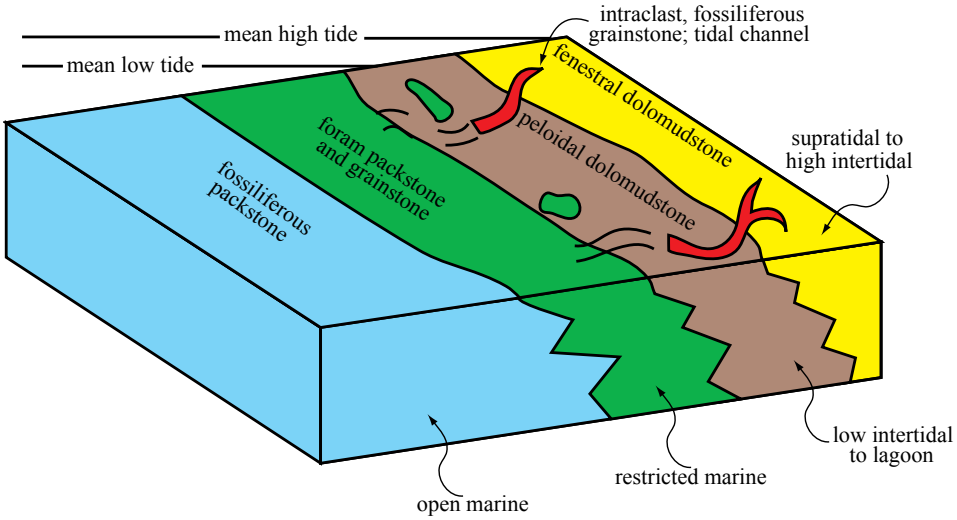

FIGURE 10—Schematic model of the distribution of carbonate lithofacies during deposition of the lower-middle Hueco transition on the Robledo Shelf. Although the foram packstone and grainstone lithofacies was probably deposited in deeper water than the peloidal dolomudstone lithofacies, the possibility that they were laterally equivalent lithofacies within the same shallow ramp or lagoon cannot be ruled out. The tidal channels (intraclast, fossiliferous grainstone lithofacies) are interpreted to have traversed the supratidal-intertidal (solid lines) and shallow subtidal (dashed lines) environments. Shale lithofacies (upper offshore marine) was either deposited seaward of the open-marine fossiliferous packstone, or was deposited during wetter paleoclimatic periods when carbonate sediment was not deposited.

maximum flooding surface is represented by heavy bioturbation that extends as much as 30 cm below the top of the uppermost carbonate bed beneath marine shale. The burrows include vertical *Diplocraterion* and *Skolithos* and large, horizontal to subhorizontal *Thallasinoides*, all of which are filled with small fossils that are not present or are rare in the host sediment (Fig. 8F). In order for the unreinforced burrows to have avoided collapse after abandonment, the host sediment must have been at least partially solidified, a condition that defines a firmground within the *Glossifungites* ichnofacies (MacEachern et al. 1992). Partial lithification of a carbonate firmground commonly is accomplished during periods of slow sediment accumulation, which is consistent with the interpretation of a maximum flooding surface. Because it overlies the maximum flooding surface, the base of the offshore marine shale was deposited in the deepest water, which is consistent with the model of Heckel (1977, 1980). However, in the context of the model of Olszewski and Patzkowsky (2003), deposition of the remainder of the shale occurs during the highstand systems tract. The shale also may reflect a change to a more humid climate and a greater influx of fine siliciclastic sediment to the sea (Fig. 11B).

Composite megasequences

Also present in the lower-middle Hueco transition are composite megasequences, which are similar to those defined by Mitchum and Van Wagoner (1991) and described in Permian rocks by Olszewski and Patzkowsky (2003). Generally meters to tens of meters thick, each composite megasequence in the study area is characterized by a lower stratal package that indicates overall deepening of the sequences and an overlying package of shallower-water or upward-shallowing sequences. Unlike the composite megasequences of Mitchum and Van Wagoner (1991) and Olszewski and Patzkowsky (2003), there is no evidence for an erosional surface at the base of the composite megasequences in the study area. Because these erosional surfaces are commonly of very low relief, they may not be recognizable within the small area of this study. The lower-middle Hueco transition has 7 composite megasequences (Fig. 5). Composite megasequences 5 and 6 are unusual compared to the others in that their deeper-water parts contain thick (4.5–7.0 m) parasequence sets.

There is considerable variation in the thickness of sequences within the composite megasequences. For example, the part of composite megasequence 1 from 11 m to 24 m contains sequences that are more than twice as thick as those immediately below. Thick sequences are also present in the upper part of composite megasequence 4 and in the lower parts of composite megasequences 5 and 6. That part of a composite megasequence that contains thick sets of sequences results from a higher than normal rate of creation of accommodation space. Because many of the intervals with thick sequences contain very shallow water carbonate facies (peloidal and fenestral dolomudstone), higher-than-normal tectonic subsidence of the Robledo Shelf and/or long-term, eustatic sea-level rise were probably critical factors in the creation of accommodation space.

Temporal scale of sequences and composite megasequences

A rough estimate of the average duration of each carbonate-shale sequence and composite megasequence can be calculated by dividing the number of sequences and composite megasequences by the approximate time span during which the lower-middle Hueco transition was deposited. In the Robledo Mountains the Hueco Formation probably spans the entire North American Wolfcampian Stage, which correlates to the Asselian, Sakmarian, and Artinskian global stages (Wardlaw et al. 2004). The Asselian ranges from 298.9 to 295.5 Ma, the Sakmarian ends at 290.1 Ma and the Artinskian ends at 279.3 Ma, totaling 19.6 m.y. (International Chronostratigraphic Chart 2012). The lower-middle Hueco transition represents 21% of the total thickness of the Hueco Formation in the Robledo Mountains (Seager et al. 2008). Assuming that sediment accumulation rate was constant during the deposition of the Hueco Formation, then the lower-middle Hueco transition would have been deposited in about 4.1 m.y. There are 49 sequences and 7 composite megasequences in the lower-middle Hueco transition, resulting in an average duration of 86,673 yrs per sequence and 585,714 yrs per composite megasequence. The duration per sequence is in the range of the fourth-order cycles of Van Wagoner et al. (1990) (about 100,000 yrs), which are assumed to result from eustatic sea-level changes associated with the waxing and waning of continental glaciers related to variations in the eccentricity of the orbit of Earth (Crowley and North 1991). Glacial-eustatic influence on sea-level cycles in the lower-middle Hueco transition is viable, because of evidence for early Permian continental

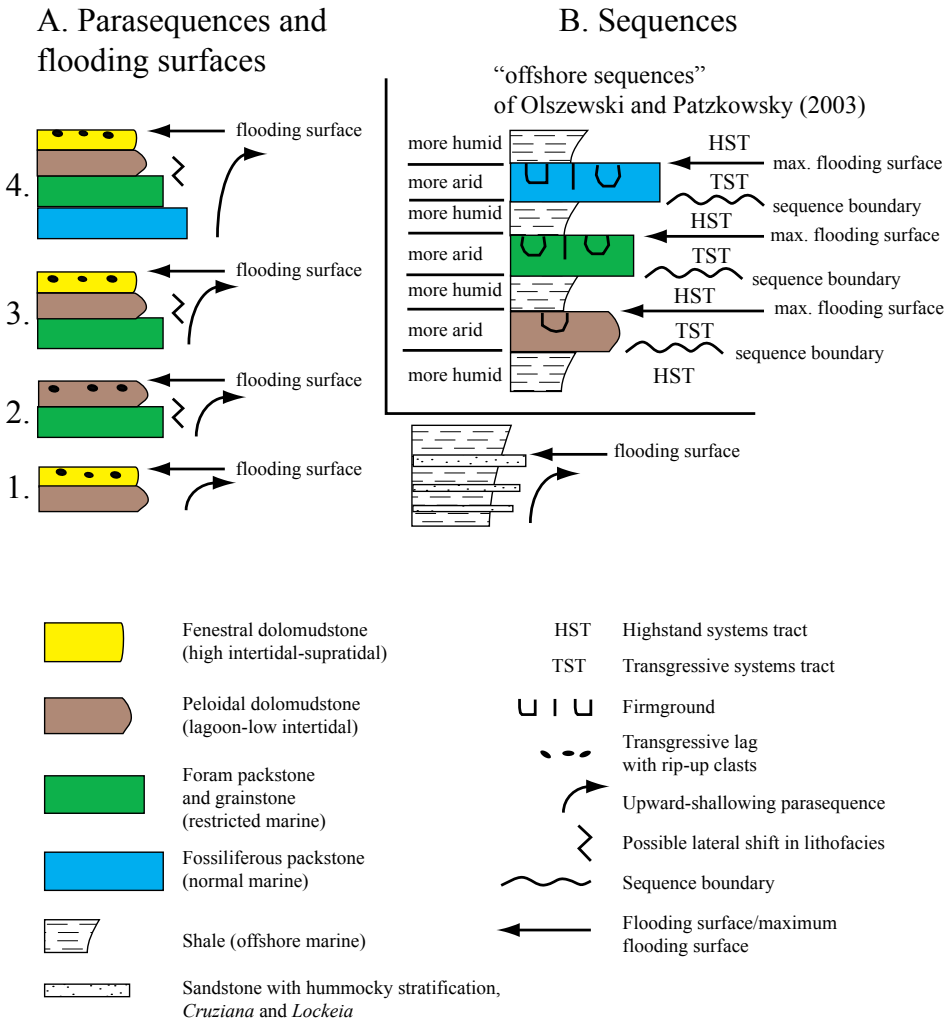

FIGURE 11—Examples of **A**—Parasequences and **B**—Carbonate-shale sequences in the lower-middle Hueco transition, Robledo Mountains.

glaciers in Antarctica and Australia (Isbell et al. 2003; Fielding et al. 2008). Based on their work in Australia, Fielding et al. (2008) defined two glacial intervals and two interglacial intervals between the beginning of the Asselian and end of the Artinskian Stages. However, at the present time biostratigraphy within the Hueco Formation in the Robledo Mountains is insufficient to allow correlation to the glacial-interglacial intervals of Fielding et al. (2008).

The average duration of each composite megasequence (about 600 k.y.) in the lower-middle Hueco transition is significantly longer than the upper limit (about 400 k.y.) of Milankovitch cycles related to orbital eccentricity (Crowley and North 1991), suggesting they may not be related to glacial eustacy. Instead, the composite megasequences may be a response to subsidence and/or to nonglacial eustacy.

Conclusions

A comparison of lithofacies and their relative abundances between the lower-middle Hueco transition and the remainder of the Hueco Formation in the Robledo Mountains provides insight into the nature of the Robledo Shelf during Wolfcampian time. The lower-middle Hueco transition contains fewer beds of open-marine limestone (fossiliferous packstone) than the upper Hueco member and the lower part of the lower Hueco member (Wahlman and King 2002), the latter of which has, in addition to fossiliferous packstone, ooid limestones and a phylloid algae bioherm as much as 6 m thick. Conversely, the lower-middle Hueco transition has a higher percentage of restricted-marine lithofacies (foram packstone and grainstone) and lagoonal to supratidal lithofacies (peloidal dolomudstone, intraclast, fossiliferous grainstone, fenestral dolomudstone) than the remainder of the formation. Taken together, this suggests that during deposition of the lower-middle Hueco transition, the Robledo Shelf experienced more restricted-marine conditions and underwent more frequent shallowing into the supratidal zone than during deposition of the rest of the formation. The most common parasequence in the lower-middle Hueco transition (peloidal dolomudstone overlain by fenestral dolomudstone, overlain by peloidal dolomudstone or deeper lithofacies) indicates frequent progradation of the carbonate shoreline across the shelf, implying that carbonate production exceeded the creation of accommodation space by sea-level rise and/or by subsidence.

Completely lacking in the lower-middle Hueco transition are fluvial-estuarine sandstones and shales, which are common in the Abo Tongue (Mack et al. 2003; Mack 2007) and present in the upper Hueco. This indicates that during deposition of the lower-middle Hueco transition, the Robledo Shelf was not traversed by a fluvial system, despite ample evidence for exposure during deposition on supratidal flats. However, deposition of marine shale was common during the lower-middle Hueco interval of time, as it was during deposition of the Abo Tongue and upper part of the middle member. These marine shales were probably derived from rivers north of the Robledo Shelf or were brought to the shelf by shore-parallel drift. In contrast, the absence or paucity of marine shales in the lower part of the lower Hueco member and in the upper Hueco member is anomalous and not understood at the present time.

Acknowledgments

This study was funded, in part, by the Institute of Tectonic Studies at New Mexico State University. Mike Pope, Gregory Wahlman, Maya Elrick, and Jane Love read an earlier version of this manuscript and made helpful suggestions for its improvement.

References

Adams, J. E., and Rhodes, M. L., 1960, Dolomitization by seepage refluxion: American Association of Petroleum Geologists, Bulletin, v. 44, pp. 1912–1920.

Ahr, W. M., 1973, The carbonate ramp, an alternative to the shelf model: Gulf Coast Association of Geological Societies, Transactions, v. 23, pp. 221–225.

Bathurst, R. G. C., 1975, Carbonate sediments and their diagenesis: Developments in Sedimentology 12, Elsevier, Amsterdam, 658 pp.

Cecil, C. B., 1990, Paleoclimate controls on stratigraphic repetition of chemical and siliciclastic rocks: Geology, v. 18, pp. 533–536.

Crowley, T. J., and North, G. R., 1991, Paleoclimatology: Oxford University Press, Oxford, U.K., 339 pp.

Curtis, R., Evans, G., Kinsman, D. J. J., and Shearman, D. J., 1963, Association of dolomite and anhydrite in the recent sediments of the Persian Gulf: Nature, v. 197, pp. 679–680.

Deffeyes, K. S., Lucia, F. J., and Weyl, P. K., 1965, Dolomitization of recent and Plio–Pleistocene sediments by marine evaporite waters on Bonaire, Netherlands Antilles; *in* Pray, L. C., and Murray, R. C. (eds.), Dolomitization and limestone diagenesis: Society of Economic Paleontologists and Mineralogists, Special Publication 13, pp. 71–88.

Durr, C. W., 2010, Early Permian sedimentation from the Robledo Shelf to the western Orogrande Basin, Robledo and Doña Ana Mountains, south-central New Mexico: Unpublished M.S. thesis, New Mexico State University, Las Cruces, 62 pp.

Enos, P., 1983, Shelf environment; *in* Scholle, P. A., Bebout, d. G., and Moore, C. H. (eds.), Carbonate depositional environments: American Association of Petroleum Geologists, Memoir 33, pp. 267–295.

Evans, G., 1966, The recent sedimentary facies of the Persian Gulf region: Philosophical Transactions of the Royal Society of London, Series A, v. 259, pp. 291–298.

Evans, G., and Bush, P. R., 1969, Some sedimentological and oceanographic observations on a Persian Gulf lagoon: U.N.E.S.C.O. Conference on Coast Lagoons, Mexico City, 1967, pp. 155–170.
Evans, G., Schmidt, V., Bush, P., and Nelson, H., 1969, Stratigraphy and geologic history of the sabkha, Abu Dhabi, Persian Gulf: Sedimentology, v. 12, pp. 145–159.
Fielding, C. R., Frank, T. D., Birgenheier, L. P., Rygel, M. C., Jones, A. T., and Roberts, J., 2008, Stratigraphic imprint of the late Paleozoic ice age in eastern Australia: A record of alternating glacial and nonglacial climate regime: Journal of the Geological Society of London, v. 165, pp. 129–140.
Heckel, P. H., 1977, Origin of phosphatic black shale facies in Pennsylvanian cyclothems ofmidcontinent North America: American Association of Petroleum Geologists, Bulletin, v. 61, pp. 1045–1068.
Heckel, P. H., 1980, Paleogeography of eustatic model for deposition of midcontinent Upper Pennsylvanian cyclothems; *in* Fouch, T. D., and Magathan, E. R. (eds.), Paleozoic paleogeography of the west-central United States, Rocky Mountain Paleogeography Symposium 1: Denver, Colorado, The Rocky Mountain Section, Society of Economic Paleontologists and Mineralogists, pp. 197–213.
Howard, J. D., and Reineck, H. E., 1981, Depositional facies of high-energy beach-to-offshore sequence: comparison with low-energy sequence: American Association of Petroleum Geologists, Bulletin, v. 65, pp. 807–830.
Illing, L. V., Wells, A. J., and Taylor, J. C. M., 1965, Penecontemporary dolomite in the Persian Gulf; *in* Pray, L. C., and Murray, R. C. (eds.), Dolomitization and limestone diagenesis: Society of Economic Paleontologists and Mineralogists, Special Publication 13, pp. 89–111.
International Chronostratigraphic Chart, 2012: International Commission on Stratigraphy, www.stratigraphy.org.
Irwin, M. L., 1965, General theory of epeiric clear water sedimentation: American Association of Petroleum Geologists, Bulletin, v. 49, pp. 445–459.
Isbell, J. L., Lenaker, P. A., Askin, R. A., Miller, M. F., and Babcock, L. E., 2003, Reevaluation of the timing and extent of late Paleozoic glaciation in Gondwana: role of the Transantarctic Mountains: Geology, v. 31, pp. 977–980.
Kendall, C. G., and Skipwith, P. A., 1969, Holocene shallow-water carbonate and evaporate sediments of Khor al Bazam, Abu Dhabi, southwest Persian Gulf: American Association of Petroleum Geologists, Bulletin, v. 53, pp. 841–869.
Kinsman, D. J. J., 1964, The recent carbonate sediments near Halat el Bahrani, Trucial Coast, Persian Gulf; *in* Van Straaten, L. M. J. U. (ed.), Deltaic and shallow marine deposits, Elsevier, Amsterdam, pp. 185–192.
Kottlowski, F. E., 1963, Paleozoic and Mesozoic strata of southwestern and south-central New Mexico: New Mexico Bureau of Mines and Mineral Resources, Bulletin 79, 100 pp.
Kottlowski, F. E., Flower, R. H., Thompson, M. L., and Foster, R. W., 1956, Stratigraphic studies of the San Andres Mountains, New Mexico: New Mexico Bureau of Mines and Mineral Resources, Memoir 1, 132 pp.
Kozur, H. W., and LeMone, D. V., 1995, The Shalem Colony section of the Abo and upper Hueco members of the Hueco Formation of the Robledo Mountains, Doña Ana County, New Mexico—stratigraphy and new conodont-based age determinations; *in* Lucas, S. G., and Heckert, A. B. (eds.), Early Permian footprints and facies: New Mexico Museum of Natural History and Science, Bulletin 6, pp. 39–55.
Kues, B. S., 1995, Marine fauna of the Early Permian (Wolfcampian) Robledo Mountains member, Hueco Formation, southern Robledo Mountains, New Mexico; *in* Lucas, S. G., and Heckert, A. B. (eds.), Early Permian footprints and facies: New Mexico Museum of Natural History and Science, Bulletin 6, pp. 63–90.
Kues, B. S., and Giles, K. A., 2004, The late Paleozoic Ancestral Rocky Mountains system in New Mexico; *in* Mack, G. H., and Giles, K. A. (eds.), The geology of New Mexico, a geologic history: New Mexico Geological Society, Special Publication 11, pp. 95–136.
Lawton, T. F., Giles, K. A., Mack, G. H., Singleton, D. S., and Thompson, A. D., 2002, Lower Wolfcampian conglomerate in the southern Caballo Mountains, Sierra County, New Mexico—stratigraphy, correlation, and implications for Late Pennsylvanian–Early Permian tectonics; *in* Lueth, V. W., Giles, K. A., Lucas, S. G., Kues, B. S., Myers, R. G., and Ulmer-Scholle, D. (eds.), Geology of White Sands: New Mexico Geological Society, Guidebook 53, pp. 257–265.
Logan, B. W., Rezak, R., and Ginsburg, R. N., 1964, Classification and environmental significance of algal stromatolites: Journal of Geology, v. 72, pp. 68–83.
Lucas, S. G., and Heckert, A. B., eds., 1995, Early Permian footprints and facies: New Mexico Museum of Natural History and Science, Bulletin 6, 301 pp.
MacEachern, J. A., Raychaudhuri, I., and Pemberton, S. G., 1992, Stratigraphic applications of the *Glossifungites* ichnofacies: delineating discontinuities in the rock record; *in* Pemberton, S. G. (ed.), Applications of ichnology to petroleum exploration: Society of Economic Paleontologists and Mineralogists, Core Workshop 17, Tulsa, Oklahoma, pp. 169–198.
Mack, G. H., 2003, Lower Permian terrestrial paleoclimatic indicators in New Mexico and their comparison to paleoclimate models; *in* Lucas, S. G., Semken, S. C., Berglof, W. R., and Ulmer-Scholle, D. (eds.), Geology of the Zuni Plateau: New Mexico Geological Society, Guidebook 54, pp. 231–240.
Mack, G. H., 2007, Sequence stratigraphy of the Lower Permian Abo member in the Robledoand Doña Ana Mountains near Las Cruces, New Mexico: New Mexico Geology, v. 29, pp. 3–12.
Mack, G. H., Leeder, M., Perez-Arlucea, M., and Bailey, B. D. J., 2003, Sedimentology, paleontology, and sequence stratigraphy of Early Permian estuarine deposits, south-central New Mexico, USA: Palaios, v. 18, pp. 403–420.
Miller, K. B., McCahon, T. J., and West, R. R., 1996, Lower Permian (Wolfcampian) paleosol-bearing cycles of the U.S. midcontinent—evidence of climatic cyclicity: Journal of Sedimentary Research, v. 66, pp. 71–84.
Mitchum, R. M., Jr., and Van Wagoner, J. C., 1991, High-frequency sequences and their stacking patterns: sequence stratigraphic evidence of high-frequency eustatic cycles: Sedimentary Geology, v. 70, pp. 131–160.
Mutti, M., and Hallock, P., 2003, Carbonate systems along nutrient and temperature gradients: some sedimentological and geochemical constraints: International Journal of Earth Science, v. 92, pp. 465–475.
Newell, N. D., Imbrie, J., Purdy, E. G., and Thurber, D. L., 1959, Organism communities and bottom facies, Great Bahama Bank: American Museum of Natural History, Bulletin, v. 117, pp. 177–228.
Olszewski, T. D., and Patzkowsky, M. E., 2003, From cyclothems to sequences: the record of eustasy and climate on an icehouse epeiric platform (Pennsylvanian–Permian, North American midcontinent): Journal of Sedimentary Research, v. 73, pp. 15–30.
Pray, L. C., 1961, Geology of the Sacramento Mountains escarpment, Otero County, New Mexico: New Mexico Bureau of Mines and Mineral Resources, Bulletin 35, 144 pp.
Purdy, E. G., 1963, Recent calcium carbonate facies of the Great Bahama Bank, 2. Sedimentary facies: Journal of Geology, v. 71, pp. 472–497.
Purdy, E. G., 1974, Karst-determined facies patterns in British Honduras: Holocene carbonate sedimentation model: American Association of Petroleum Geologists, Bulletin, v. 58, pp. 825–855.
Rankey, E. C., 1997, Relations between relative changes in sea level and climate shifts—Pennsylvanian–Permian mixed carbonate-siliciclastic strata, western United States: Geological Society of America, Bulletin, v. 109, pp. 1089–1100.
Schneider, J. F., 1975, Recent tidal deposits, Abu Dhabi, United Arab Emirates, Arabian Gulf; *in* Ginsburg, R. N. (ed.), Tidal deposits, a casebook of recent examples and fossil counterparts: Springer-Verlag, New York, pp. 209–214.
Scholle, P. A., and Ulmer-Scholle, D. S., 2003, A color guide to the petrography of carbonate rocks: grains, textures, porosity, diagenesis: American Association of Petroleum Geologists, Memoir 77, 474 pp.
Seager, W. R., 1981, Geology of Organ Mountains and southern San Andres Mountains, New Mexico: New Mexico Bureau of Mines and Mineral Resources, Memoir 36, 97 pp.
Seager, W. R., and Mack, G. H., 2003, Geology of the Caballo Mountains, New Mexico: New Mexico Bureau of Geology and Mineral Resources, Memoir 49, 136 pp.
Seager, W. R., Kottlowski, F. E., and Hawley, J. W., 1976, Geology of Doña Ana Mountains, New Mexico: New Mexico Bureau of Mines and Mineral Resources, Circular 147, 36 pp.
Seager, W. R., Kottlowski, F. E., and Hawley, J. W., 2008, Geologic map of the Robledo Mountain and vicinity, New Mexico: New Mexico Bureau of Geology and Mineral Resources, Open-file Report 509, 12 pp.
Shaw, A. B., 1964, Time in stratigraphy: McGraw-Hill, New York, 365 pp.
Shinn, E. A., 1968, Practical significance of birdseye structures in carbonate rocks: Journal of Sedimentary Petrology, v. 38, pp. 215–223.
Shinn, E. A., 1983, Tidal flat environment; *in* Scholle, P. A., Bebout, d. G., and Moore, C. H. (eds.), Carbonate depositional environments: American Association of Petroleum Geologists, Memoir 33, pp. 171–210.
Shinn, E. A., Ginsburg, R. N., and Lloyd, R. M., 1965, Recent supratidal dolomite from Andros Island, Bahamas; *in* Pray, L. C., and Murray, R. C. (eds.), Dolomitization and limestone diagenesis: Society of Economic Paleontologists and Mineralogists, Special Publication 13, pp. 112–123.
Soreghan, G. S., 1997, Walther's law, climate change, and upper Paleozoic cyclostratigraphy in the Ancestral Rocky Mountains: Journal of Sedimentary Research, v. 67, pp. 1001–1004.
Stoklosa, M. L., Simo, J. A., and Wahlman, G. P., 1998, Facies description and evolution of a Wolfcampian (Early Permian) shelf margin: Hueco Mountains, west Texas; *in* Mack, G. H., Austin, G. S., and Barker, J. M. (eds.), Las Cruces country II: New Mexico Geological Society, Guidebook 49, pp. 177–186.
Tandon, S. K., and Gibling, M. R., 1994, Calcrete and coal in late Carboniferous cyclothems of Nova Scotia, Canada—climate and sea-level changes linked: Geology, v. 22, pp. 755–758.
Vail, P. R., Mitchum, R. M., and Thompson, S., 1977, Seismic stratigraphy and global changes of sea level, part 3: relative changes of sea level from coastal onlap; *in* Payton, C. E. (ed.), Seismic stratigraphy—applications to hydrocarbon exploration: American Association of Petroleum Geologists, Memoir 26, pp. 63–82.
Van Wagoner, J. C., Posamentier, H. W., Mitchum, R. M., Vail, P. R., Sarg, J. F., Loutit, T. S., and Hardenbol, J., 1988, An overview of the fundamentals of sequence stratigraphy and key definitions; *in* Wilgus, C. K., Hastings, B. S., Kendall, C. G., Posamentier, H. W., Ross, C. A., and Van Wagoner, J. C. (eds.), Sea-level changes—an integrated approach: Society of Economic Paleontologists and Mineralogists, Special Publication 42, pp. 39–45.
Van Wagoner, J. C., Mitchum, R. M., Campion, K. M., and Rahmanian, V. D., 1990, Siliciclastic sequence stratigraphy in well logs, cores, and outcrops—concepts for high-resolution correlation of time and facies: American Association of Petroleum Geologists, Methods in Exploration Series, No. 7, 55 pp.
Vasconcelos, C., and McKenzie, J. A., 1997, Microbial mediation of modern dolomite precipitation and diagenesis under anoxic conditions (Lagoa Vermelha, Rio de Janeiro Brazil): Journal of Sedimentary Research, v. 67, pp. 378–390.
Wahlman, G. P., and King, W. E., 2002, Latest Pennsylvanian and earliest Permian fusulinid biostratigraphy, Robledo Mountains and adjacent ranges, south-central New Mexico: New Mexico Bureau of Geology and Mineral Resources, Circular 208, 26 pp.
Wardlaw, B. R., Davydov, V., and Gradstein, F. M., 2004, The Permian Period; *in* Gradstein, F. M., Ogg, J. G., and Smith, A. G. (eds.), A geologic time scale 2004, Cambridge University Press, pp. 249–270.
Wetzel, J. L., and Aigner, T., 1986, Stratigraphic completeness—tiered trace fossils provide a measuring stick: Geology, v. 14, pp. 234–237.
Wilson, J. L., and Jordan, C., 1983, Middle shelf environment; *in* Scholle, P. A., Bebout, d. G., and Moore, C. H. (eds.), Carbonate depositional environments: American Association of Petroleum Geologists, Memoir 33, pp. 297–343.